Questioning Degree of Accuracy Offered by the Spectral Element Method in Computational Electromagnetics

I. Mahariq [1,2], H. Kurt [2], and M. Kuzuoğlu [3]

[1] Department of Electrical and Electronics Engineering
University of Turkish Aeronautical Association, Ankara 06790, Turkey

[2] Department of Electrical and Electronics Engineering
TOBB University of Economics and Technology, Ankara 06560, Turkey

[3] Department of Electrical and Electronics Engineering
Middle East Technical University, Ankara 06531, Turkey
ibmahariq@gmail.com, hkurt@etu.edu.tr, kuzuoglu@metu.edu.tr

Abstract ─ In this paper, a comparison amongst the spectral element method (SEM), the finite difference method (FDM), and the first-order finite element method (FEM) is presented. For the sake of consistency, the comparison is carried out on one-dimensional and two-dimensional boundary value problems based on the same measure of error in order to emphasize on the high accuracy gained by the SEM. Then, the deterioration in the accuracy of the SEM due to the elemental deformation is demonstrated. Following this, we try to answer the question: Do we need the high accuracy offered by the SEM in computational electromagnetics? The answer is supported by solving a typical, unbounded electromagnetic scattering problem in the frequency domain by the SEM. Domain truncation is performed by the well-known perfectly matched layer (PML).

Index Terms ─ Deformation, electromagnetic scattering, finite difference, finite element, photonic nanojet, spectral element method.

I. INTRODUCTION

Spectral element method was first introduced by Patera [1] in 1984 for computational fluid dynamics. Patera proposed a spectral element method that combines the flexibility of the finite element method (FEM) with the accuracy of spectral methods (the case where *p*-type method is applied for a single-element domain). In the spectral element method, he utilized high-order Lagrangian polynomial interpolant over Chebyshev collocation points in order to represent the velocity in each element in the computational domain.

Generally speaking, spectral element methods are considered as a family of approximation schemes based on the Galerkin method. They share common characteristics with finite-element discretizations, and this provides the reason why they can be viewed as *h*- or *p*-versions of FEM. That is, when viewed as *h*-version (mesh refinement), a Lagrangian interpolation formula on the parent element exists in both, as well as the basis functions have local support. On the other hand, spectral element methods use high-degree polynomials on a fixed geometric mesh for the sake of enhanced accuracy, and this is the fact characterizing the *p*-version (order refinement) of FEMs [2].

Orthogonality of basis functions either in the *h*- or *p*-versions of the FEM is due to non-overlapping local functions. However, in spectral element methods orthogonality is related to both analytical nature and topological nature (local extension) of the basis functions. This fact tells us why spectral element method is different from the FEM of *h*-version or *p*-version [3].

There are mainly two implementations that have been proposed; one is based on the Chebyshev polynomials [1], and the other is based on the Legendre polynomials. In both cases, Gauss-Lobatto quadrature grid is utilized to perform Lagrangian interpolation. This implementation ensures the continuity of the solution and benefit from the associated numerical quadrature schemes. Patera [1] chose Chebyshev polynomials basically because of the possibility of using fast transform techniques. On the other side, the stiffness and mass matrices were evaluated by the quadratures that were performed analytically without utilizing the weighting factor associated with Chebyshev polynomials [2], (the weighting factor is $1/\sqrt{1-x^2}$, by which Chebyshev polynomials are orthogonal in contrast to Legendre polynomials whose orthogonality comes with unity weighting factor). In

Submitted On: January 12, 2015
Accepted On: June 18, 2015

this study, the implementation of SEM is based on Legendre polynomials and Gauss-Lobatto-Legendre quadrature grid is utilized to perform Lagrangian interpolation.

In computational electromagnetics, the first- or second-order FEM and the finite difference method are extensively used in numerical modeling of electromagnetic radiation and/or scattering problems, both in frequency and time domains. On the other hand, although it is known for its high accuracy [4-7], the spectral element method is not familiar to the community of electromagnetics. However, to attract the attention of the community, a consistent comparison illustrating the accuracy of these numerical methods will have a remarkable value.

In this paper, domain truncation is performed by the perfectly matched layer (PML) [8], namely the systematic formulation provided by Kuzuoglu and Mittra [9]. Based on that formulation, Mahariq, et al. [10], provided the values of the attenuation factors for the PML when SEM is utilized in modeling of frequency-domain electromagnetic problems while persevering the high accuracy of SEM.

There are three main goals of the current study. The first is to demonstrate the accuracy of the SEM, the 3-node-stencil FDM and the first-order FEM. For this purpose, a comparison is carried out by solving some boundary value problems in one dimension and two dimensions based on the same measure of error. After emphasizing on the accuracy of SEM, we illustrate the deterioration in the accuracy of SEM due to the irregularity in the elemental shapes (deformed elements). The third goal of this paper is to demonstrate a typical electromagnetic scattering problem which best provides an unusual answer to the title of the current study, i.e., does an electromagnetic problem requires the high accuracy gained by using the SEM?

The paper is arranged as follows: in Section II, a comparison amongst SEM, FDM and FEM is provided. In Section III, the deterioration in the SEM accuracy due to the elemental deformation is demonstrated. Section IV provides a typical electromagnetic scattering problem solved by the SEM, and finally some conclusions are presented in Section V.

II. ON THE ACCURACY OF SEM, FDM AND FEM

To get an insight about the accuracy gained from SEM, when compared to other numerical methods, demonstrations are performed using numerical examples. For this purpose, a comparison is first carried out between SEM and FDM with a stencil composed of 3 nodes in one dimension. We considered the following one-dimensional boundary-value problem:

$$\frac{d^2u}{dx^2}+k^2u=0,\ \text{in the interval}\,[0,1.1], \tag{1}$$

with $u(0)=1,\ u(1.1)=\exp(-jk1.1)$, where $k=2\pi$. We define an error measure as follows:

$$Err=\max_i \frac{\left|u_{i,exact}-u_{i,numerical}\right|}{\left|u_{i,exact}\right|}, \tag{2}$$

where $u_{i,exact}$ is the exact solution (for this problem, it is $\exp(-jkx)$), and $u_{i,numerical}$ is the numerical solution obtained by the specified numerical method at the ith node in the computational domain. This definition of the error measure is used throughout this paper.

In Table 1, the maximum relative errors for both FDM and SEM are presented as the number of nodes (N) increases in both methods. Obviously, it can be observed that the errors of FDM are slowly decaying although the number of nodes is chosen in the order of 10. On the other hand, SEM shows high accuracy with much fewer number of nodes. That is, the accuracy obtained by FDM at 100 nodes can be achieved by 8 nodes with SEM.

Table 1: Maximum relative errors of FDM and SEM for the problem defined in Eq. 1

FDM		SEM	
N	*Err*	N	*Err*
10	0.1840	7	0.0103
20	0.0524	8	0.0012
30	0.0238	9	1.455e-04
40	0.0135	10	1.608e-05
50	0.0087	11	2.074e-06
60	0.0060	12	2.308e-07
70	0.0044	13	2.570e-08
80	0.0034	14	2.624e-09
90	0.0027	15	2.613e-10
100	0.0022	16	2.420e-11
110	0.0020	17	2.318e-12

To compare SEM with the first-order FEM, we consider the following 1D problem:

$$\begin{aligned}&\frac{d^2u}{dx^2}+u=0,\ \text{in}\,[-1,0],\ \text{and}\\ &\frac{d^2u}{dx^2}+4^2u=0,\ \text{in}\,[0,1]\\ &\text{with}\ u(-1)=\sin(-1),\ u(1)=\sin(4).\end{aligned} \tag{3}$$

In fact, the solution of (3) is $u(x)=\sin(\mathrm{c}\,x)$, with $\mathrm{c}=1$ in $[-1,0]$, and $\mathrm{c}=4$ in $[0,1]$. However, for error calculations, to avoid division by zero, we compute the error (only for this problem) as the maximum difference between the exact solution and the numerical solution.

The comparison is shown in Table 2, in which N represents the number nodes in each sub-domain. Again, it can be seen that SEM accuracy is much higher than that of FEM. Figure 1 shows the plot of the solution obtained by SEM for 15 nodes in each subdomain.

Table 2: Maximum errors of FEM and SEM for the problem defined in Eq. 3

FEM		SEM	
N	*Err*	N	*Err*
10	0.0546	7	7.033e-05
20	0.0252	8	3.340e-06
30	0.0164	9	4.697e-07
40	0.0121	10	1.876e-08
50	0.0096	11	2.593e-09
60	0.0080	12	9.092e-11
70	0.0068	13	1.132e-11
80	0.0059	14	3.481e-13
90	0.0053	15	3.941e-14
100	0.0047	16	1.587e-14

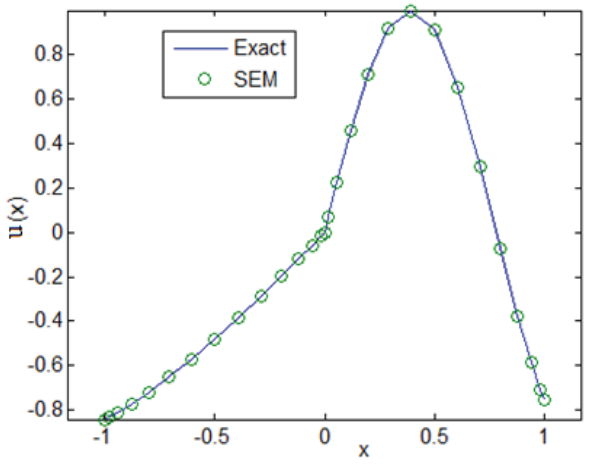

Fig. 1. Exact and SEM solutions of the problem defined in Eq. 3.

It is worth also to compare FEM and SEM in a two dimensional boundary value problem. For this purpose, the point source problem (2D Green's function) is considered. This problem is governed by the Helmholtz equation:

$$\nabla^2 u + k^2 u = -\delta(\vec{r}), \tag{4}$$

where $k = 2\pi / \lambda$, and λ is the wavelength. To avoid the singularity at the origin, the homogenous Helmholtz equation is solved inside a square element (Ω) of dimensions $\lambda \times \lambda$ and $\lambda = 1$, and Ω is defined in the xy-plane so that the point (0,0) does not belong to this element. On the boundary $\partial\Omega$, the exact to (4), which is expressed in terms of Hankel function of the second kind zero order is as follows: $(u(\vec{r}) = (j/4)H_0^{(2)}(k\,|\,\vec{\mathrm{r}}\,|)$, is applied as boundary conditions, where $|\,\vec{\mathrm{r}}\,|$ is the euclidean distance from the origin to a point $\vec{\mathrm{r}}$ on the boundary $\partial\Omega$. Right-triangle elements are utilized in meshing the problem. Figure 2 shows the solution obtained by FEM at a grid of 20×20 nodes. As observed from Table 3, the error profile in 2D does not differ from that of 1D case.

It can be clearly observed from the demonstrated numerical problems that the accuracy of SEM is much higher than that of FDM or FEM. However, it is important to study the deterioration in the accuracy of SEM when deformed elements are used to discretize a given problem. This aspect is discussed in the next section.

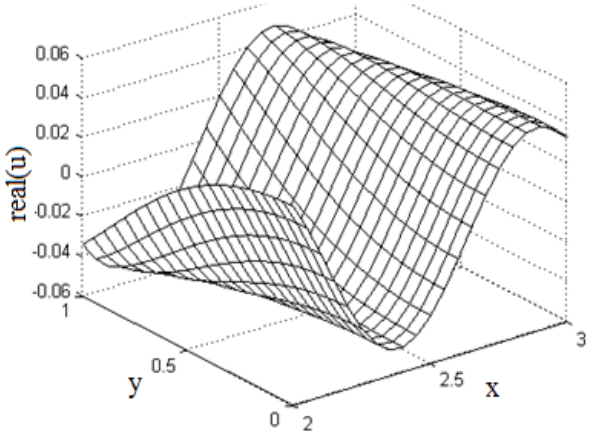

Fig. 2. FEM solution of the 2D point source problem defined in Eq. 4.

Table 3: Maximum relative errors of FEM and SEM for the problem defined in Eq. 4

FEM		SEM	
N	*Err*	N	*Err*
10	0.5554	7	0.00091
15	0.3229	8	1.30E-04
20	0.2018	9	1.25E-05
25	0.1356	10	1.14E-06
30	0.0967	11	1.13E-07
35	0.0724	12	1.26E-08
40	0.0562	13	1.51E-09
45	0.0447	14	2.23E-10
50	0.0364	15	2.57E-11
55	0.0302	16	3.23E-12
60	0.0255	17	2.86E-13
80	0.0145		
100	0.0103		

III. ELEMENTAL DEFORMATION

Most of practical engineering problems encounter

complex geometries; hence, the computational domain requires to be discretized into irregular elements. Meshing a problem in the case of FEM has been intensively investigated in the literature. For instance, if triangular elements are used to mesh a problem, it is recommended that the smallest angle in the element should not be lower than 15° in order not to deteriorate the accuracy. Hence, it is important to study the effect of elemental deformation on the accuracy in the case of SEM. In this section, we demonstrate the accuracy of spectral element method for a single-element domain of quadrilateral deformed elements.

In SEM, mapping an irregular element to the standard element (see Fig. 3) is required in order to perform the differential and integration operations involved in the process of approximating the partial differential equations by SEM. As mentioned above, the nodal basis for the standard element is usually built by Lagrangian basis polynomials associated with a tensor product grid of Gauss-Legendre-Lobatto (GLL) nodes. Figure 4 shows such a grid for a ninth-order polynomial space. As seen from Fig. 3, the flexibility in the shapes of elements can be utilized in meshing complex geometries where different scattering objects of arbitrary shapes are involved.

In this work, to differentiate between a reference square element and an irregular element, the following definition for the elemental aspect ratio (AR) is considered:

$$AR = \frac{\max(d_i)}{\min(d_i)}, \tag{5}$$

where d_i $(1 \le i \le 4)$ stands for side length of a quadrilateral element and $i = 1,2,3,4$. To make use of this definition, one needs to study the accuracy of SEM for a single-element domain having a reference area with equal dimensions (1×1). We call such an element as a reference element. Then, by changing the dimensions and the shape of the element while having the same area as that of the reference element, a comparison can be performed. With this approach, the effect of AR on the accuracy can be realized. It is also worth to note that all sides of the element have equal nodes as GLL is utilized.

The point source problem introduced in (4) is considered for this purpose. The maximum relative errors are presented in Table 4 as N increases for the reference square element and for a quadrilateral element of unit area for the aspect ratios: 1.33, 1.88, and 2.87. The real part of the solution in the straight-sided quadrilateral element is shown in Fig. 5 for AR=2.87. As seen from Table 4, the effect of the aspect ratio on the accuracy can be clearly observed. However, even at large deformation (i.e., at AR=2.87), SEM still provides much higher accuracy than its counterparts (FDM and FEM) at much coarser grids.

In terms of the presented accuracy of SEM, one may wonder whether such a high accuracy is required in order to successfully model an electromagnetic problem or not. In the next section, we try to answer such questioning.

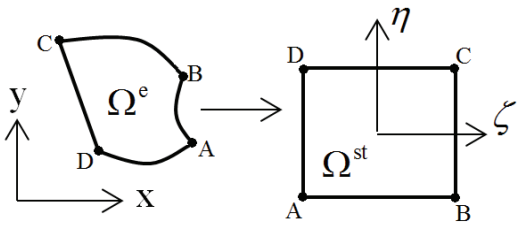

Fig. 3. Mapping an element Ω^e to the standard element Ω^{st}.

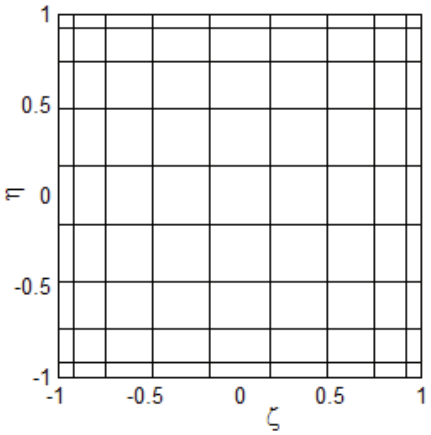

Fig. 4. GLL grid nodes on the standard element for a ninth-order polynomial space (nodes are represented by the intersections of horizontal and vertical lines).

Table 4: Maximum relative errors of SEM for the reference element and the straight-sided quadrilateral element having unit area

N	Ref. Elmt.	Straight-Sided Element		
		AR = 1.33	AR = 1.88	AR = 2.87
	Err	*Err*	*Err*	*Err*
7	9e-4	1e-3	3e-3	6e-2
8	1e-4	2e-4	6e-4	1e-2
9	1e-5	2e-5	1e-4	4e-3
10	1e-6	2e-6	3e-5	1e-3
11	1e-7	2e-7	5e-6	3e-4
12	1e-8	2e-8	8e-7	6e-5
13	1e-9	2e-9	1e-7	2e-5
14	2e-10	3e-10	2e-8	3e-6
15	3e-11	3e-11	4e-9	7e-7
16	3e-12	4e-12	6e-10	2e-7
17	3e-13	4e-13	8e-11	3 e-8

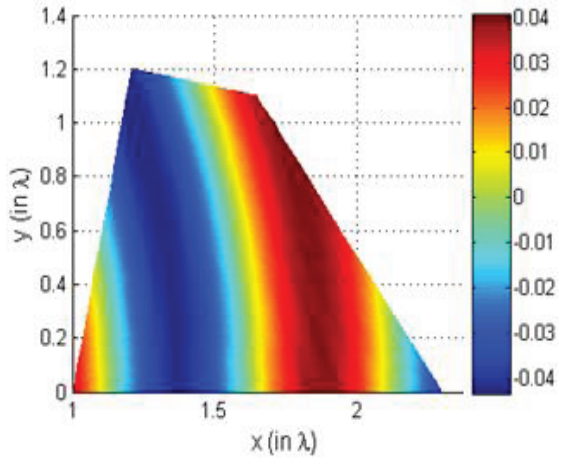

Fig. 5. SEM solution for the straight-sided quadrilateral element at AR=2.87.

IV. SCATTERING PROBLEM IN RESONANCE ELEMENTS

Accuracy of numerical approach is crucial in order to capture the intrinsic property of resonances of optical cavities. We specifically take two-dimensional dielectric micro-cylinder in this section of the study to emphasize the importance of fine discretization of the computational domain.

When an electromagnetic plane wave is incident perpendicularly to a dielectric cylinder or to a dielectric sphere, instead of having a shadow region behind the dielectric material, a photonic nanojet is obtained at some specific choices of material dimensions and a corresponding refractive index. In order to obtain a photonic nanojet, the dielectric microspheres or micro cylinders must be lossless dielectric materials and of diameters greater than the illuminating wavelength [11-15]. The phenomenon is named as photonic nanojet, due to the unique nature of the light distribution at the focal area. In Ref. 17, we provided detailed formulation of SEM and applied the method for investigating plane wave interaction with dielectric micro-cylinder.

In the case of photonic nanojet where the scatterer is assumed to be an infinitely-long dielectric cylinder, the problem can be considered as a two-dimensional one when an incident plane wave propagating in a direction perpendicular to the cylinder axis is assumed. We consider an incident plane wave propagating in the x-direction and the electric field is polarized in the z-direction (i.e., in a transverse magnetic mode, TM_z):

$$E_z^{inc} = \hat{a}_z \exp(-jkx). \tag{6}$$

To solve the problem numerically, one must truncate the unbounded domain. In this work, domain truncation is performed by the perfectly matched layer, namely using the formulation presented in [10]. Figure 6 shows in the xy-plane, a dielectric cylinder represented by Ω_C, free space region represented by Ω_{FS}, and the PML region denoted by Ω_{PML}, which represents the region surrounding Ω_{FS}.

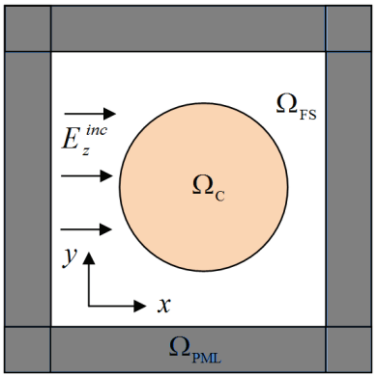

Fig. 6. Definition of the computational domain composed of a dielectric micro-cylinder (Ω_C) embedded in the free space (Ω_{FS}) and truncated by PML [17].

The set of the partial differential equations governing this electromagnetic scattering problem can be written as follows:

$$\nabla.\Lambda\nabla \mathrm{u} + \mathrm{a}\,\varepsilon_r k^2\,\mathrm{u} = k^2\left(1-\varepsilon_r\right)E_z^{inc}, \tag{7}$$

in which Λ is a tensor defined as:

$$\Lambda = \begin{bmatrix} \Lambda_{11} & 0 \\ 0 & \Lambda_{22} \end{bmatrix}, \tag{8}$$

where ε_r is the relative permittivity of the cylinder, $\mathrm{a} = 1 + \dfrac{\alpha}{\mathrm{jk}}$, α is the attenuation factor,

$\begin{bmatrix}\Lambda_{11} & \Lambda_{22}\end{bmatrix} = \begin{bmatrix}\dfrac{1}{\mathrm{a}} & \mathrm{a}\end{bmatrix}$ for x-decay in the PML region,

$\begin{bmatrix}\Lambda_{11} & \Lambda_{22}\end{bmatrix} = \begin{bmatrix}\mathrm{a} & \dfrac{1}{\mathrm{a}}\end{bmatrix}$ for y-decay in the PML region,

$\begin{bmatrix}\Lambda_{11} & \Lambda_{22}\end{bmatrix} = \begin{bmatrix}\dfrac{1}{\mathrm{a}} & \dfrac{1}{\mathrm{a}}\end{bmatrix}$ for a corner (xy-decay) in the PML region with $\mathrm{a}=1$ in Ω_{FS}, and ε_r being greater than 1 in Ω_{SC} only, and 1 elsewhere. If n denotes the refractive index of the cylinder, then $n^2 = \varepsilon_r$.

It is worth to mention that, after obtaining the solution by spectral element method, which represents the scattered field, the incident plane wave is added to the scattered field in the subdomains Ω_C and Ω_{FS} only. One can produce the same spatial light distribution for the case where FDTD method is used. We have performed FDTD study and verified the exact photonic nanojet generation. With the application of SEM in the frequency domain, it is easy to decompose

the total field into incident and scattered field components. Figure 7 shows the visualization of photonic nanojet when the cylinder radius is $R = 5.0\lambda$ and dielectric constant is $n = 1.30$.

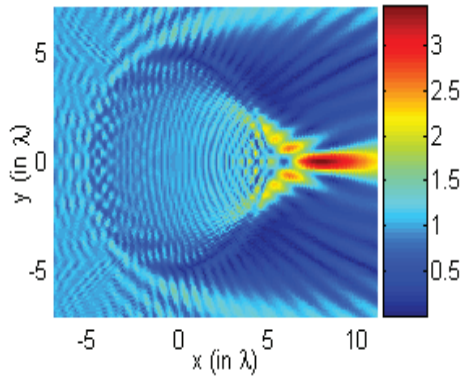

Fig. 7. Visualization by the SEM of photonic nanojet at $R = 5.0\lambda$ and $n = 1.30$.

Figure 8 shows one of the captured resonance mode supported by a dielectric micro cylinder with $R = 3.5\lambda$ and $n = 1.70$. The light focusing action with small amplitude can be observed at the interior part of the dielectric cylinder. On the other hand, strong electric field localization at around the small cylinder appears with a highly symmetric light distribution in the form of two rings. Light is trapped at the circumference of the cylinder by the total internal reflection mechanism.

The special case corresponding to specific radius and refractive index values in Fig. 8 can be attributed to whispering gallery mode (WGM). In the representation of WGM, m indicates the azimuthal mode number, and l represents the radial mode number. Using this notation we can express Fig. 8 in terms of WGM resonances. By means of spectral element method, we captured resonance modes as well as photonic nano jets cases as the details are reported in Ref. [17].

Photonic nanojet analysis can also be performed analytically. The well-known Mie theory was intensively utilized in electromagnetic scattering problems. However, when the characteristic dimensions of the scattering object becomes much larger than the wavelength, improper algorithms may lead to considerable numerical errors [16]. In the examples presented in the previous section, where resonance behavior takes places, the diameter of the micro-cylinder is larger than the wavelength but not too much. It is very important to check whether the analysis that Mie theory provides produces such resonance cases or not. Itagi and Challener [16] provided the solution of the scattered light by a dielectric cylinder using Mie theory. This analytical solution is used to verify the existence of WGM in scattering by dielectric microcylinders. Figure 9 presents the scattered field inside the cylinder at $R = 3.5\lambda$. The good match between Fig. 8 and Fig. 9 can be observed clearly.

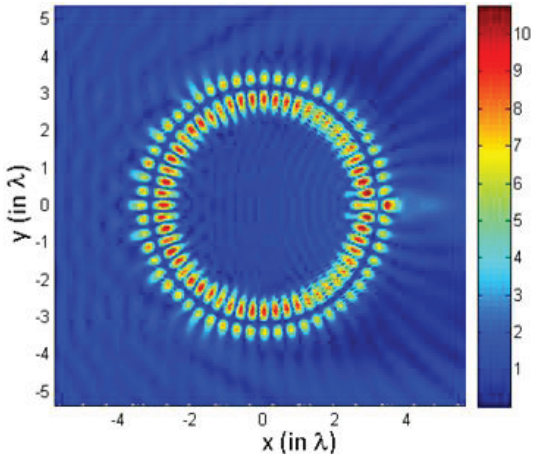

Fig. 8. Visualization of the evolution of a photonic nano-jet for $R = 3.5\lambda$ and $n = 1.70$. Whispering gallery mode representation gives $l = 2$ and $m = 28$ [17].

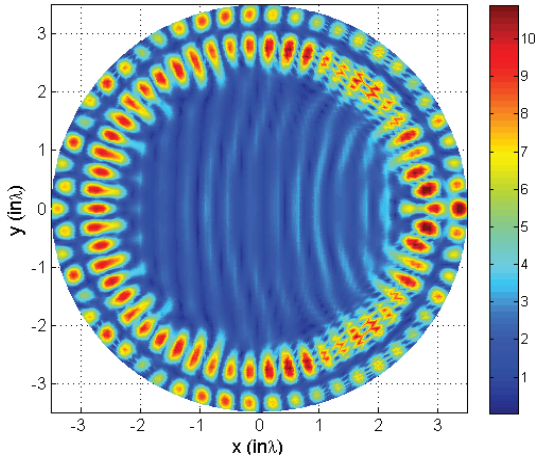

Fig. 9. The analytical solution in Ω_C visualizes the WGM ($l = 2$ and $m = 28$) for the case shown in Fig. 8.

With the use of SEM, we could accurately perform field analysis of photonic nanojets in dielectric lossless micro cylinders. Strong light focusing at the shadow side of the micro-cylinder is reported. Advantageous features of SEM allow the observation of commonly reported nanojet scenarios as well as the least pointed out transition region where resonance mode appears under certain conditions. The creation of whispering gallery mode types is plainly observed.

Two dimensional dielectric cylinders may act either as resonant or focusing element depending on the stimulating conditions. One cannot observe and capture resonance frequencies if the discretization of the

computational domain is not properly performed. As an example, we provide field distribution of the dielectric cylinder under the same parameters ($n=1.70$ and $R=3.5\lambda$) except the case that low resolution (16×16 nodes are assigned for each element) is introduced. Compared to Fig. 8, we see that the resonance is lost as shown in Fig. 10.

Depending on the nature of the resonance mode (spectrally how sharp or broad the mode) one should utilize even finer or coarse discretization in the computational method as in SEM. Consequently, capturing of resonance requires fine discretization of the computational domain.

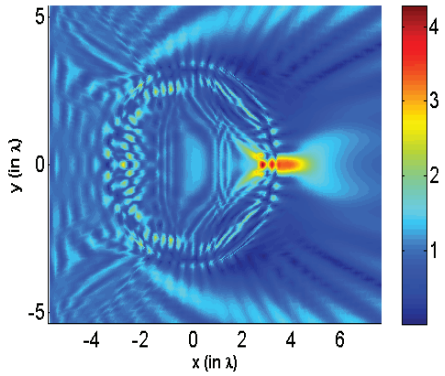

Fig. 10. Visualization of the evolution of a photonic nanojet for $R=3.5\lambda$ and $n=1.70$ at 16×16 nodes per element. WGM behavior is destroyed due to low resolution.

V. CONCLUSION

To realize and appreciate the accuracy of spectral element method, we carried out a comparison between this method and its well-known counter parts such as FDM and FEM. For this purpose, we applied these numerical methods to solve specific problems and the corresponding error calculations are subjected to a specific error measure. From the illustrated examples, it is clear that the accuracy of spectral element method is much higher than that of its counter parts.

In most of practical engineering problems, the geometry of the region of interest is irregular. This means that discretization of the problem into elements of regular shapes is impossible. Spectral element method gives the capability of using deformed elements; and hence, a freedom in modeling irregular problems. For this reason, we illustrated the accuracy of this numerical method for single-deformed element case in order to check the deterioration of the elemental deformation on the accuracy of SEM. The aspect ratio of the element is considered as a measure of the deformation with fixed area. Based on the illustrations, we conclude that the accuracy of SEM even with large elemental deformation (which should be avoided while meshing an electromagnetic problem) still dominates the accuracy achieved by FDM or FEM.

The accuracy of the spectral element method is very high as it can be observed from the presented numerical demonstrations. Here, it is important to ask the following interesting question: What would be the order of the error while solving a computational problem? One may seek an accuracy at around 10^{-2} or 10^{-3} while designing a system to capture the general behavior of the device. Hence, low-order FEM or FDM are very suitable and do meet some engineering purposes. However, based on the electromagnetic scattering problem discussed in Section IV, the answer to the above question has to be modified: we do indeed need high accuracy in some cases, especially resonance characteristics require fine resolution. That is, when low-order numerical methods are used to study electromagnetic scattering by dielectric microspheres or micro cylinders, whispering gallery mode will be missed. So, if the engineer design the material based on the numerical solution from a low-order method, and if whispering gallery mode takes place in the final implementation, the whole design will be in jeopardy.

ACKNOWLEDGMENT

The first author acknowledges the financial support from Technical Research Council of Turkey (TUBITAK). Kurt acknowledges partial support from the Turkish Academy of Sciences.

REFERENCES

[1] A. T. Patera, “A spectral element method for fluid dynamics: Laminar flow in a channel expansion,” *Journal of Computional Physics*, vol. 54, pp. 468-488, 1984.

[2] M. O. Deville, P. F. Fischer, and E. H. Mund, *High-Order Methods for Incompressible Fluid Flow*, Cambridge University Press, vol. 9, 2002.

[3] G. Karniadakis and S. Sherwin, *Spectral/hp Element Methods for Computational Fluid Dynamics*, Oxford University Press, 2013.

[4] J. Lee, T. Xiao, and Q. H. Liu, “A 3-D spectral-element method using mixed-order curl conforming vector basis functions for electromagnetic fields,” *IEEE Trans. on Microwave Theory and Techniques*, vol. 54-1, pp. 437-444, Jan. 2006.

[5] J. Lee and Q. H. Liu, “A 3-D spectral-element time-domain method for electromagnetic simulation,” *IEEE Trans. on Microwave Theory and Technique*, vol. 55-5, pp. 983-991, May 2007.

[6] O. Z. Mehdizadeh and M. Paraschivoiu, “Investigation of a two-dimensional spectral element method for Helmholtz’s equation,” *Journal of Computational Physics*, vol. 189, pp. 111-129, 2003.

[7] S. J. Hesthaven, S. Gottlieb, and D. Gottlieb, *Spectral Methods for Time-Dependent Problems*, Cambridge University Press, 2007.
[8] J. P. Berenger, "A perfectly matched layer for the absorption of electromagnetic waves," *Journal of Computational Physics*, vol. 114, pp. 185-200, 1994.
[9] M. Kuzuoglu and R. Mittra, *A Systematic Study of Perfectly Matched Absorbers*, Frontiers in Electromagnetics, IEEE Press, 2000.
[10] I. Mahariq, M. Kuzuoglu, and I. H. Tarman, "On the attenuation of the perfectly matched layer in electromagnetic scattering problems with the spectral element method," *Applied Computational Electromagnetics Society Journal*, vol. 29.9, pp. 701-710, 2014.
[11] Z. Chen, A. Taflove, and V. Backman, "Photonic nanojet enhancement of backscattering of light by nanoparticles: a potential novel visible-light ultramicroscopy technique," *Optics Express*, vol. 12, pp. 1214-1220, 2004.
[12] S. Lecler, Y. Takakura, and P. Meyrueis, "Properties of a three-dimensional photonic jet," *Optics Lett*., vol. 30 (19), pp. 2641-2643, 2005.
[13] A. Devilez, B. Stout, N. Bonod, and E. Popov, "Spectral analysis of three-dimensional photonic jets," *Optics Express*, vol. 16, pp. 14200-14212, 2008.
[14] P. Ferrand, J. Wenger, A. Devilez, M. Pianta, B. Stout, N. Bonod, E. Popov, and H. Rigneault, "Direct imaging of photonic nanojets," *Optics Express*, vol. 16, pp. 6930-6940, 2008.
[15] M.-S. Kim, T. Scharf, S. Mühlig, C. Rockstuhl, and H. P. Herzig, "Engineering photonic nanojets," *Optics Express*, vol. 19, pp. 10206-10220, 2011.
[16] A. V. Itagi and W. A. Challener, "Optics of photonic nanojets," *Journal of Optics Society*, vol. 22, no. 12, 2005.
[17] I. Mahariq, M. Kuzuoglu, I. H. Tarman, and H. Kurt, "Photonic nanojet analysis by spectral element method," *IEEE Photonics Journal*, 6, 6802714 (2014).

Ibrahim Mahariq took his B.Sc. degree from the department of Electrical and Computer Engineering/ Palestine Polytechnic University in 2003. He worked there as Teaching Assistant during 2003-2005. He received the M.Sc. in Design of Electrical Machines, and his Ph.D. in Computational Electromagnetics from Middle East Technical University, Ankara, Turkey. Mahariq was granted TUBITAK scholarship for his Ph.D. studies in 2010. Mahariq is currently working on Photonics to earn his second Ph.D. in the department of Electrical and Electronics Engineering at TOBB University of Economics and Technology, Ankara, Turkey. Mahariq is currently serving as an Assistant Professor at the University of Turkish Aeronautical Association, Department of Electrical and Electronics Engineering.

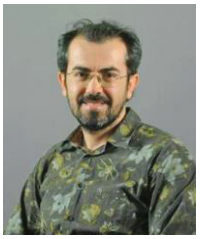

Hamza Kurt received the B.S. degree from Middle East Technical University, Ankara, Turkey, in 2000, the M.S. degree from the University of Southern California, Los Angeles, CA, USA, in 2002, and the Ph.D. degree from the Georgia Institute of Technology (Georgia Tech), Atlanta, GA, USA, in 2006, all in Electrical and Electronics Engineering. He was a Research Fellow with the Cedars-Sinai Medical Center, Bio-photonics Research Lab, Los Angeles, from 2001 to 2002. He spent a year with the Institut d'Optique Graduate School, Paris, France, as a Post-Doctoral Scientist. Since December 2007, he has been with the TOBB University of Economics and Technology, Ankara, as an Associate Professor with the Electrical and Electronics Engineering Department. He has authored more than 50 research papers in refereed international journals.

His current research interests include nanophotonics including the design and analysis of nanophotonic materials and media for the realization of wavelength-scale optical elements, slow light structures, graded index optics, high-resolution imaging, polarization insensitive devices, optical cavities/waveguides, and optical biosensors. Kurt is a Member of the Optical Society of America and IEEE Photonics Society.

Mustafa Kuzuoglu received the B.Sc., M.Sc., and Ph.D. degrees in Electrical Engineering from Middle East Technical University (METU), Ankara, Turkey, in 1979, 1981, and 1986, respectively. He is currently a Professor with METU. His research interests include computational electromagnetics, inverse problems, and radars.